Journal of Applied Mechanics and Technical Physics, Vol. 42, No. 3, pp. 404–410, 2001

NOTES ON GAS-DYNAMIC DESIGN OF SUPERSONIC FLYING VEHICLES

G. I. Maikapar

UDC 531.3+537.8

It is shown that the lift-to-drag ratio of a thin delta wing is significantly lower than the lift-to-drag ratio of an infinitely long swept plate with an identical lift force. The effect of sweep on a finite wing may be used by excluding disturbances from the leading edge of the wing via introducing a "hardened" stream surface (wedge) and increasing the wing length. A three-shock waverider is proposed for choosing the optimal parameters. The sharp wedge may be avoided by replacing planar shock waves by a cylindrical shock wave upstream of the blunted wedge. If the leading edge of the wedge is not parallel to the rib that is a source of the expansion wave, a plate with zero wave drag, generating a lift force, may be obtained behind this rib. The system of regularly intersecting shock waves may be applied to design a forward-swept wing.

Choosing the shape of supersonic flying vehicles is the subject of numerous studies (particularly, in the U.S.A.). The shape of the vehicle or the shock wave attached to the leading edges is specified parametrically, and the variational problem is solved numerically, using exact or approximate equations of motion of the gas. Another widely used method is the gas-dynamic design, which implies composing of the surface of the flying vehicle from parts of stream surfaces of known flows behind shock waves and expansion waves [1–3]. The advantage of this method is the goal-oriented choice of gas flows for which exact solutions of equations of motion are available, the simplicity of calculations, and the smaller number of parameters sufficient to meet the restrictions imposed on the volume, size, moment, and other parameters during optimization. Adverse effects (separation) are eliminated, deviations (in practice) from the optimal shape (edge bluntness) do not lead to principal changes in aerodynamic characteristics, and the flow structure is retained in the case of small deviations from the design regime.

We consider the problem of reduction of the wave (inductive) drag for a given lift force for a thin plane wing with a shock wave attached to the leading edge. We consider only the main part of the lift force generated by the windward side of the wing, i.e., we assume that the leeward side is formed by an undisturbed stream surface passing through the leading edge. For comparison, we take an infinitely long plate of finite width, which is normal to the xy plane (the x axis is directed along the free-stream velocity V and the y axis is opposite to the lift force). The edge of the plate makes an angle Λ with the xy plane. The lift-to-drag ration of the plate is

$$K = \left\{ \frac{7\,\mathrm{M}^2/25}{(p_2/p_1 - 1)^2} \left[6\,\frac{p_2}{p_1} + 1 + \frac{(6 + p_2/p_1)^2}{7\,\mathrm{M}_1^2 - (6p_2/p_1 + 1)} \right] - 1 \right\}^{1/2}$$

(the ratio of heat capacities is assumed to be 7/5). Here M_1 is the Mach number for the velocity component normal to the leading edge upstream of the shock wave, M is the free-stream Mach number, p_2/p_1 is the ratio of pressures upstream and downstream of the shock wave (for a delta wing and a conical waverider, p_2 is the pressure averaged over the area). The angle of attack α, the flow deflection behind the shock wave δ, and the value of Λ are related as $\sin\alpha = \mathrm{M}_1 \sin\delta/\mathrm{M}$ and $\sin\Lambda = \tan\alpha/\tan\delta$.

Figure 1 shows the lift-to-drag ratio K of the plate versus the pressure ratio p_2/p_1, which is equivalent to the dependence of K on the lift force if the projection of the wing area onto the y axis is prescribed, for M = 3

Joukowski Central Aerohydrodynamic Institute, Zhukovskii 140180. Translated from Prikladnaya Mekhanika i Tekhnicheskaya Fizika, Vol. 42, No. 3, pp. 24–31, May–June, 2001. Original article submitted February 1, 2000; revision submitted June 8, 2000.

 0021-8944/01/4203-0404 $25.00

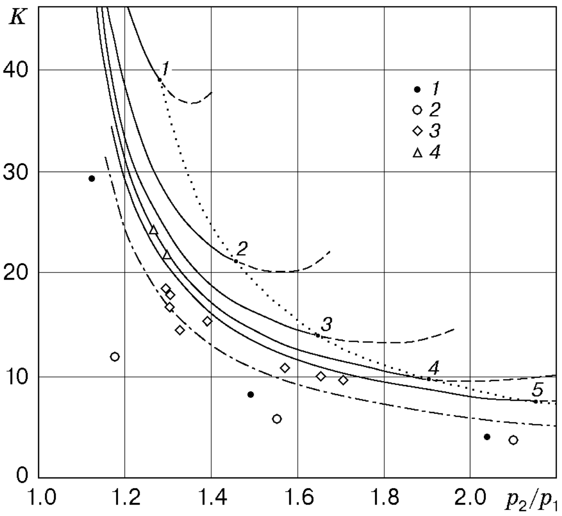

Fig. 1. Lift-to-drag ratio of wings versus the lift force for $M_1 = 1.2$ and $\Lambda = 23.8°$ (curve 1); $M_1 = 1.3$ and $\Lambda = 25.5°$ (curve 2), $M_1 = 1.4$ and $\Lambda = 27.5°$ (curve 3), $M_1 = 1.5$ and $\Lambda = 29.5°$ (curve 4), and $M_1 = 1.6$ and $\Lambda = 31.4°$ (curve 5); the solid and dashed curves refer to an infinitely long plate for $M_2 > 1$ and $M_2 < 1$, respectively, the dotted curve refers to a "limiting" plate, AND the dot-and-dashed curve refers to a triangular plate, Nonweiler wing, or right wedge ($\Lambda = \pi/2$); the points refer to a conical waverider ($\beta_C = 5$, 10, and 15°) (1), the cone generatrix ($\beta_c = 5$, 10, and 15°) (2), a forward-swept wing normal to the xy plane (3), and a wing with zero drag (4).

(M_2 is the Mach number for the normal component of velocity behind the shock wave). For high Mach numbers, the calculation results are qualitatively similar.

The above formula demonstrates the positive influence of slipping: an increase in K with decreasing angle Λ for a given lift force p_2/p_1. As for a cone and a finite-length wedge, the actual limit for an infinite swept plate is $M_2 = 1$, since perturbations from the trailing edge reach the shock wave at $M_2 < 1$, which is incompatible with the boundary conditions on the shock wave. The lift-to-drag ratio of a triangular plate calculated by the linear theory depends only on the Mach number and on the lift coefficient C_y and is independent of the angle Λ [4].

Based on the results of systematic calculations (numerical solution of the Euler equations [5]), we obtained the approximate formula for the mean pressure at the lower surface of the delta wing

$$\frac{\langle p\rangle_{\text{lower}}}{p_\infty} = 1 + \frac{1.4\,\mathrm{M}^2\alpha}{\sqrt{\mathrm{M}^2 - 1}}\,[1 + 0.01\,\mathrm{M}\,(57.3\alpha)^{1\,+\,0.015\mathrm{M}}],$$

from which IT follows that the lift-to-drag ratio of the triangular plate ($K = \cot\,\alpha$) calculated by the nonlinear theory depends only on the Mach number and lift force. The pressure calculated by this formula equals the pressure behind the shock wave $\Lambda = \pi/2$. This allows us to calculate the wave drag of pyramids with faces in the form of isosceles triangles, which may be significantly lower than the drag of cones of an identical volume. The lift-to-drag ratio of the triangular plate is significantly lower than the lift-to-drag ratio of the "limiting" plate ($M_2 = 1$); the Nonweiler wing (waverider) [6] and the right wedge with side washers ($\Lambda = \pi/2$) [7] have the same lift-to-drag ratio (Fig. 1).

On the delta wing, the effect of the swept wing [8] is compensated by the pressure decrease in its central part. The pressure increase associated with this effect corresponds to regions behind the shock waves between the edges and characteristics emanating from the wing tip. These regions disappear at $M_2 = 1$. To preserve this effect, it is necessary to prevent penetration of perturbations from the wing beginning (plane of symmetry or airframe/wing junction) to the flow region behind the shock wave, which may be done by adding the "hardened" stream surface beginning at the shock wave and reaching the wing surface. This surface may be a plane. As a result, we obtain a waverider with two planar shock waves attached to the edges of the wing and the centerbody (wedge).

There are more possibilities for choosing the optimal parameters in considering the waverider with three planar shock waves (Fig. 2), which has the wing OFDC (the angle of flow deflection in the shock wave is δ_2) and the airframe OABC (the angle of flow deflection in the central shock wave is δ_1) (the x axis is directed along the

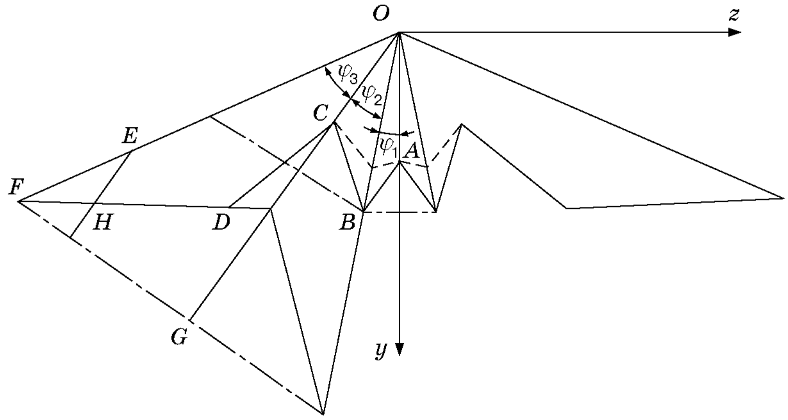

Fig. 2. Projection of the waverider with three planar shock waves onto the yz plane: the dashed curves refer to the trailing edges of the wedge and dot-and-dashed curves refer to the lines of intersection of shock waves with the yz plane.

free-stream velocity). We note an interesting feature of the flow behind the side shocks: the "hardened" stream planes passing through the vectors of the free-stream velocity and the flow behind the shock wave may generate a lift force in the case of zero drag. This plane is the normal-to-shock wing OCG ($\varphi_3 = 0$). The end of the wing with the lift force other than zero, which is bent along the streamline behind the shock wave EH whose plane is normal to the shock wave, has zero drag also (Fig. 2). The lift-to-drag ratio of a constant-width and finite-length plate with the same bent ends (swept wedge with washers) is the same as the lift-to-drag ratio of an infinite plate, but the total lift force of the wing ends equals zero if the trailing edges of the washers are identical. For an identical length of the wing and airframe, the lift-to-drag ratio of the waverider is

$$K = \Big\{1 + \frac{\cos(\varphi_1 + \varphi_2)}{\sin\varphi_1}\,[\sin\varphi_2 + \cos\varphi_2 \tan\,\varphi_3(1 - a^2)]\Big\}\Big\{\tan\,\delta_1 + \frac{\tan\,\delta_2}{\sin\varphi_1}\,[\sin\varphi_2 + \cos\varphi_2 \tan\,\varphi_3(1 - a^2)]\Big\}^{-1},$$

where a is the length of the chord of the bent end EH. If the pressure behind the shock waves is identical ($\delta_1 = \delta_2$), then the lift-to-drag ratio is maximum at $\varphi_1 + \varphi_2 = 0$, i.e., in the case of the Nonweiler wing. Hence, the effect of the swept wing is not manifested on the waverider considered either because of the presence of the wedge.

For a waverider with an axisymmetric conical shock attached to the wing edges, the wings of zero drag are meridional planes, the additional surface is the airframe (a sector of a cone) [9], and the lift-to-drag ratio is maximum in the case of a half-cone. However, the lift-to-drag ratio of this waverider is lower than the lift-to-drag ratio of a delta wing and approaches the latter only if the cone half-angle $\beta_{\rm c}$ is small, when the wing area is much greater than the projection of the cone area onto the y axis (see Fig. 1). The local lift-to-drag ratio on the lower generatrix of the cone ($\cot\,\beta_{\rm c}$) is even smaller than the lift-to-drag ratio of the waverider considered above; though the value of K increases (simultaneously with decreasing pressure) along the streamline from the cone to the shock wave, it equals the lift-to-drag ratio behind the planar shock wave only on the shock wave itself. Therefore, we cannot say that the waverider designed from a conical shock has a better lift-to-drag ratio than the waverider constructed using a planar shock. The volume of the half-cone is significantly smaller than the volume of the Nonweiler wing or a delta wing with the leeward side formed by free-stream planes. We can also add that concave transverse contours of the wings were obtained in solving variational problems, and the shock wave is closer to planar rather than to conical [10, 11].

Obviously, the effect of the swept wing may be achieved only by using wings of greater length than that of the airframe. If the airframe has a bottom, the side edge of the wing CD (Fig. 2) should be located outside of the region of propagation of disturbances from the bottom edge or coincide with the boundary of this region. If the wedge-bottom edge BC is straight, the region of weak perturbations emanating from it is bounded by characteristic cones with apices at the points B and C and planes enveloping cones with apices at points of the straight line BC [12]. In the coordinate system with the origin at the point C, the x axis directed along the streamline, the y axis directed opposite to the lift force, and the z axis directed toward the shock wave, the tangent of the angle of

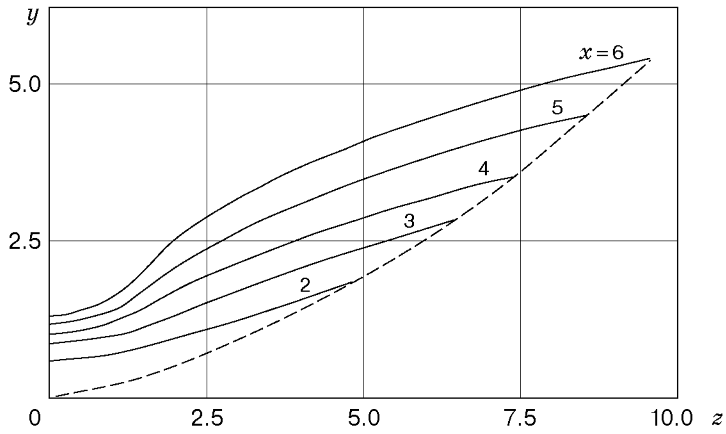

Fig. 3. Cross-sectional contours of the waverider with a cylindrical shock wave attached to the leading edge (the dashed curve is the line of intersection of the wave by a horizontal plane).

inclination of the line of intersection of the envelope with the wing plane λ to the x axis is

$$\frac{\tan\lambda}{m} = \frac{k\sqrt{k^2 + l^2 - m^2} - ml}{k^2 - m^2}.$$

Here $k = dy/dx$ and $l = dz/dx$ are the tangents of the angles of inclination of the trailing edge of the wedge and $m = \sqrt{(\mathrm{M}^2 + 5)/[1 + \mathrm{M}_1^2(1 - v_2^2)/5] - 6}$ is the tangent of the angle of inclination of the characteristic to the streamline [$v_2 = \cos\theta_2/\cos(\theta_2 - \delta_2)$ is the ratio of the normal components of velocity downstream and upstream of the shock wave, where θ_2 is the angle of inclination of the shock wave]. For $x > 0$, $k > 0$, and $l \leqslant m$ and $x < 0$, $k < 0$, and $l \leqslant -m$, the region of propagation of disturbances is bounded by the characteristic $\tan\alpha = m$; otherwise, it is bounded by the envelope. If the edge is located in the yz plane and $dz/dy > 0$, then we have $\tan\delta/m = \sqrt{1 + (dz/dy)^2}$. The region of flow retaining behind the shock is expanded with distance from the origin if $\gamma - \lambda > 0$; the leading and side edges are parallel for $\gamma = \lambda$. In both cases, this region is infinite. The region is constricted and has a finite length for $\gamma - \lambda < 0$ [γ is the angle between the leading edge and the streamline behind the shock; $\tan\gamma = v_2/\sqrt{(\mathrm{M}/\mathrm{M}_1)^2 - 1}$]. It should be noted that the length of wings of the waverider with a conical shock is limited, since the characteristic crosses the shock wave. In the presence of a wedge, the case $\mathrm{M}_2 < 1$ is realistic [13], but the optimum in the lift-to-drag ratio is more probable for $\mathrm{M}_2 > 1$, since the wing does not become narrower and the wedge is smaller in the latter case. An increase in the wing length and a decrease in the wedge area owing to the addition of a third shock and inclination of the trailing edges (dashed curves in Fig. 2) allow us to approach the lift-to-drag ratio of the "limiting" plate. The problem should be solved taking into account technical conditions for the vehicle and the friction force.

Several interacting wings may be used for a limited length.

A sharp wedge may be avoided by using a gas flow behind a cylindrical shock wave upstream of an infinite swept wedge with circular bluntness; the results for a planar flow can be found in [14]. Figure 3 shows the cross-sectional contours of the windward side of the waverider formed by streamlines behind the bow shock wave of a blunted wedge with an angle of 20°, passing through the plane leading edge, which is the line of intersection of the wave by a horizontal plane (dashed curve). The dimensions in Fig. 3 are normalized to the bluntness radius of the wedge. The x axis (the critical line of the wave) is inclined to the free-stream direction at an angle $\Lambda = 41.8°$, the y axis is located in the plane of symmetry of the wedge, and the Mach number is $\mathrm{M} = 3$. With increasing x, there appears an airframe smoothly transformed into a flat wing, as in the case of a waverider with two planar shocks. The lift force and drag of the waverider are readily calculated via the components of the force acting on the windward side:

$$X = \iint (p - p_1)\,dy\,dz, \qquad Y = p_1 V\cos\Lambda \iint (\sin\Lambda - v)\,dy\,dz.$$

Here v is the projection of velocity onto the y axis; the limits of integration are the trailing edge and its projection onto the bow shock wave.

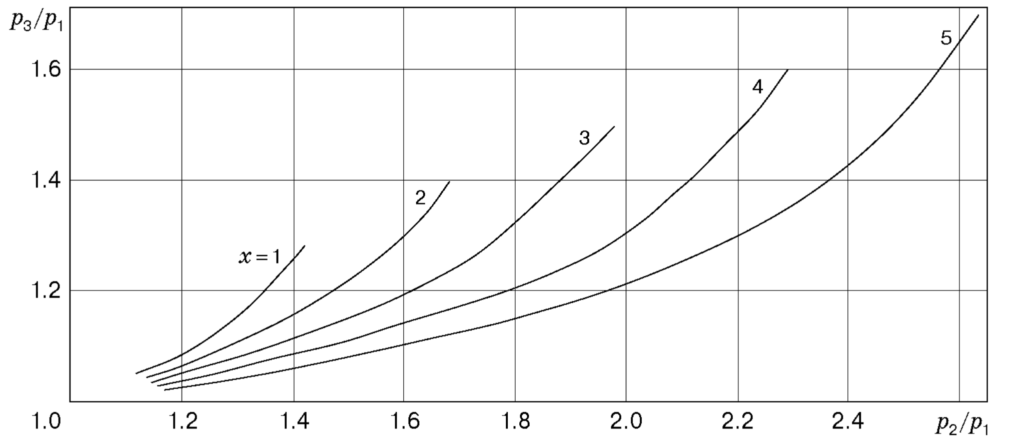

Fig. 4. Pressure behind the expansion wave on the plane with zero angle of attack (the curves for the cross sections $x = 1$, 2, 3, 4, and 5 correspond to the values of the parameters M_1 and Λ for curves 1–5 in Fig. 1).

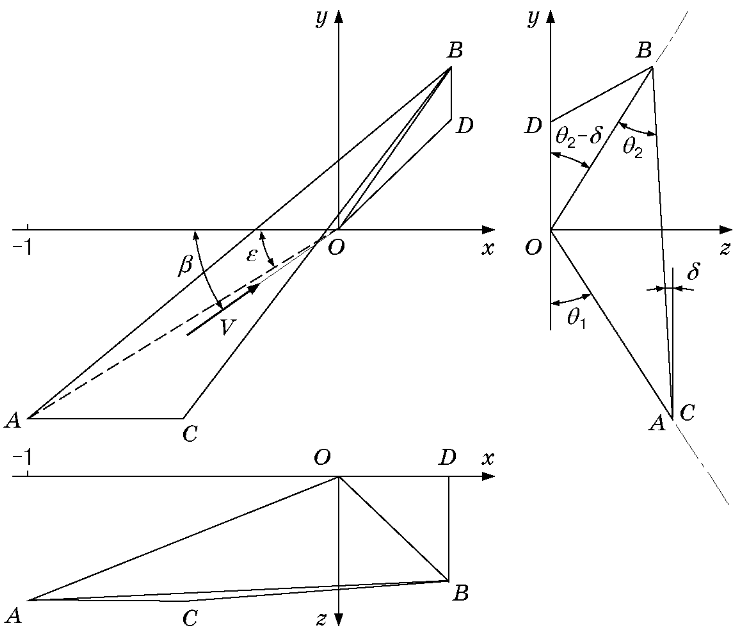

Fig. 5. Projections of the forward-swept wing of low aspect ratio with a system of crossing shock waves attached to the leading edges.

For the configuration "wedge–plate" with a shock wave attached to the leading edge of the wedge and an expansion wave emanating from the junction of the wedge with the plate (hinge or inflection), for a zero angle of attack of the plate, the pressure on the latter p_3 for $\mathrm{M} > 3$ and wedge angles lower than $10°$ differs insignificantly from the pressure upstream of the shock wave p_1 ("underexpansion" [15]); regimes of "overexpansion" are not considered here. This condition is also valid in the case of a swept wing, if the line of inflection is parallel to the leading edge, in accordance with the principle of independence [16]. However, if the line of inflection is normal to the streamline behind the shock wave and the angle of deflection Δ is such that the angle of attack of the deflected plane is equal to zero, i.e., $\tan\Delta = \tan\alpha/\cos(\Lambda-\gamma)$, $\tan\gamma = v_2/\sqrt{(\mathrm{M}/\mathrm{M}_1)^2-1}$, and the Mach number upstream of the expansion wave is $\mathrm{M}_3 = \mathrm{M}_1 v_2/\sin\gamma$, then we have $p_3 > p_1$. The excessive pressure behind the line of inflection $p_3/p_1 - 1$ is rather high as compared to the pressure behind the shock wave $p_2/p_1 - 1$ (Fig. 4), which may be used to generate the lift force with zero drag. The region of the pressure p_3 is limited by the characteristic passing from the point of intersection of the leading edge and the line of inflection.

We consider a system of regularly intersecting weak planar shock waves for designing a forward-swept wing (the lift-to-drag ratio of the backward-swept wing with such a system of shocks is significantly lower than the lift-to-drag ratio of a delta wing [7]). An interesting feature of the forward-swept wing, in particular, is that it may be calculated using the exact solution for an expansion flow with two waves and a tractor fin [17]. We direct the x axis along the line of intersection of shock waves (Fig. 5). The leading edge of the wing (plate) is located on the first shock wave OA, and its position is set by the angle ε so that we have $y/x = \tan\varepsilon$ and $z/x = -\tan\varepsilon\tan\theta_1$. The streamline behind the first shock emanates from the end of the edge A, which forms the side edge AB. The second boundary of the wing is the line of its intersection with the second shock OB. The line OB and the streamline behind the second shock OD form the plane of the central wedge. To retain the flow behind the first shock, an additional solid surface (fin) is needed; its plane passes through the side edge of the wing and the line of intersection of the shock wave with the vertical plane AC. The trailing edge of the fin CB is assumed to be swept to reduce the drag of the fin (the drag of the outer side equals zero, and the base drag is ignored). The flow velocity is directed at an angle β to the x axis; the quantities marked by subscripts 1, 2, and 3 and corresponding to the velocity components ahead of the first shock, behind it, and ahead of the second shock are

$$V_{x1} = V_{x2} = V_{x3} = V\cos\beta, \qquad V_{y1} = V\sin\beta, \qquad V_{z1} = 0,$$

$$V_{y2} = Vv_2\sin\beta\cos\delta, \qquad V_{z2} = -Vv_2\sin\beta\sin\delta, \qquad v_2 = \cos\theta_1/\cos(\theta_1-\delta),$$

$$V_{y3} = Vv_2v_3\sin\beta, \qquad V_{z3} = 0, \qquad v_3 = \cos\theta_2/\cos(\theta_2-\delta).$$

The equation of the wing plane is

$$\frac{\sin(\theta_1-\delta)}{\cos\theta_1}\,x - \Big(\frac{\tan\theta_1}{v_2\tan\beta} - \frac{\sin\delta}{\tan\varepsilon}\Big)y + \Big(\frac{\cos\delta}{\tan\varepsilon} - \frac{1}{v_2\tan\beta}\Big)z = 0,$$

the tangent of the line of its intersection with the xy plane is

$$\Big(\frac{y}{x}\Big)_0 = \frac{\sin(\theta_1-\delta)}{\sin\theta_1/(v_2\tan\beta) - \sin\delta\cos\theta_1/\tan\varepsilon},$$

and the angle of attack is $\alpha = \beta - \arctan(y/x)_0$.

We consider two variants of the wing geometry: 1) the wing is normal to the xy plane [$\tan\varepsilon = (y/x)_0 = v_2\tan\beta\cos\delta$] and the lines AO and AB projected onto the xy plane coincide; 2) the wing is normal to the first shock wave, and its drag equals zero; the wing passes through the free-stream line [$(y/x)_0 = \tan\beta$ and $\tan\varepsilon = \tan\beta\cos^2\theta_1$]. The case of coincident planes of the wing and wedge is also possible $(y/x)_0 = v_2v_3\tan\beta$, but it is not considered here, since the lift-to-drag ratio of the wing is equal to the lower lift-to-drag ratio of the wedge. The point B has the coordinates

$$x_{\rm B} = \frac{\sin(\theta_1-\delta)\cos(\theta_2-\delta)}{\sin\theta_2\cos\theta_1}, \qquad y_{\rm B} = \frac{\tan\beta\tan(\theta_1-\delta)\cos(\theta_2-\delta)}{\sin\theta_2}$$

in the first variant and

$$x_{\rm B} = \frac{\sin(\theta_1-\delta)\cos(\theta_1+\theta_2-\delta)}{\sin\theta_2}, \qquad y_{\rm B} = \frac{\tan\beta\cos\theta_1\sin(\theta_1-\delta)\cos(\theta_2-\delta)}{\sin\theta_2}$$

in the second variant. In both cases, we have $z_{\rm B} = y_{\rm B}\tan(\theta_2-\delta)$. The trailing edge of the fin is assumed to be sonic, and the length of its leading edge AC is

$$a = \frac{l\sin\mu_2}{\sin(\gamma+\mu_2)}, \qquad \cos\gamma = \frac{1}{\sqrt{1+v_2^2\tan^2\beta}}.$$

Here μ_2 is the characteristic angle behind the first shock wave and l is the length of the line AB.

To eliminate perturbations from the line of intersection of the characteristic cone with the apex at the point C and the second shock, we locate the trailing edge of the wedge BD in the plane normal to the xy plane; the coordinate of the point D is $y_{\rm D} = x_{\rm B}v_2v_3\tan\beta$. The lift force and the drag of the wing with the wedge and fin are calculated from the areas of projections of the xz and yz planes, using the coordinates of the points A, B, C, and D. The calculation results for M = 3, $\beta = 27$–$42°$, and $\delta = 4$–$8°$ are plotted in Fig. 1. Only for the second variant of the wing geometry is the lift-to-drag ratio of the wing of low aspect ratio significantly greater than the lift-to-drag ratio of the delta wing; therefore, taking into account the large area of the fin, it should be rather considered as an entrance part of the inlet. With increasing aspect ratio (decreasing l), the lift-to-drag ratio approaches the lift-to-drag ratio of an infinite plate.

REFERENCES

1. V. A. Shchepanovskii, *Gas-Dynamic Design* [in Russian], Nauka, Novosibirsk (1991).
2. V. A. Shchepanovskii and B. I. Gutov, *Gas-Dynamic Design of Supersonic Inlets* [in Russian], Nauka, Novosibirsk (1993).
3. Yu. A. Vedernikov and V. A. Shchepanovskii, *Optimization of Gas-Dynamic Systems* [in Russian], Nauka, Novosibirsk (1995).
4. A. Ferri, *Elements of Aerodynamics of Supersonic Flows*, Macmillan, New York (1949).
5. G. P. Voskresenskii, A. S. Il'ina, and V. S. Tatarenchik, "Supersonic flow around wings with an attached shock wave," *Tr. TsAGI*, No. 1590 (1974).
6. D. Küchemann, *The Aerodynamic Design of Aircraft*, Pergamon Press, Oxford (1978).
7. G. I. Maikapar, "Waveriders of complex shape," *Izv. Ross. Akad. Nauk, Mekh. Zhidk. Gaza*, No. 4, 158–165 (1998).
8. A. Busemann, "Lift force at supersonic velocities," in: *Gas Dynamics* [Russian translation], GONTI, Moscow (1939), pp. 143–177.
9. V. V. Keldysh, "Lift-to-drag ratio of a conical sector with a wing in regimes corresponding to sectors of the flow in the vicinity of a circular cone at a zero angle of attack," *Izv. Ross. Akad. Nauk, Mekh. Zhidk. Gaza*, No. 6, 118–121 (1968).
10. V. N. Golubkin, D. S. Emelin, and D. S. Postnov, "Problems of wing optimization under conditions typical of supersonic flight," *Tr. TsAGI*, No. 2636, 38–41 (1998).
11. S. A. Takovitskii, "Optimization of a delta wing with transverse and longitudinal curvature and a great number of varied parameters," *Tr. TsAGI*, No. 2636, 98–105 (1988).
12. V. V. Keldysh, "Favorable wing/body interference at supersonic velocities," *Uch. Zap. TsAGI*, **2**, No. 1, 17–23 (1971).
13. Yu. I. Zaitsev and V. V. Keldysh, "Special cases of flow near a supersonic edge and the line of intersection of shock waves," *Uch. Zap. TsAGI*, **1**, No. 1, 43–89 (1970).
14. M. G. Lebedev, L. V. Pchelkina, and I. D. Sandomirskaya, *Supersonic Flow Around Blunted Bodies* [in Russian], Izd. Mosk. Univ., Moscow (1974).
15. V. L. Grigorenko and A. N. Kraiko, "Internal shock waves in a supersonic perfect-gas flow around wedge–plate and cone–cylinder configurations," *Prikl. Mat. Mekh.*, **50**, No. 1, 91–103 (1986).
16. R. T. Jones, *Wing Theory*, Princeton Univ. Press, New Jersey (1990).
17. G. I. Maikapar, "Shape of the leeward side of the waverider," *Uch. Zap. TsAGI*, **16**, No. 2, 9–16 (1985).